Contribution from the Istituto di Chimica Generale e Inorganica,
Università, Laboratorio CNR, Florence, Italy

Synthesis and Structural Characterization of Some Nitrosyl Complexes of Iron, Cobalt, and Nickel with Poly(tertiary phosphines and arsines)

M. DI VAIRA, C. A. GHILARDI, and L. SACCONI*

Received November 18, 1975 AIC50834K

The tripodlike ligands tris(2-diphenylphosphinoethyl)amine, np$_3$, and tris(2-diphenylarsinoethyl)amine, nas$_3$, having the donor atom sets NP$_3$ and NAs$_3$, respectively, form metal nitrosyl complexes with the formula [M(NO)L]X (M = Fe, Co, Ni; L = np$_3$, nas$_3$; X = I, NO$_3$, BF$_4$, BPh$_4$) and the neutral complex [Co(NO)(np$_3$)]. Complete x-ray analyses performed on the three [M(NO)(np$_3$)]BPh$_4$ complexes have shown that the iron complex has a trigonal-bipyramidal geometry whereas the cobalt and nickel complexes are tetrahedral, the central nitrogen atom of the ligand in these cases being not coordinated. The MNO group is essentially linear in the three complexes, although results for the iron and cobalt complexes are affected by some uncertainty, due to the bad quality of the data. Structural, magnetic, and spectral data are discussed on the basis of a simple molecular orbital approach.

Introduction

Many attempts have so far been made to correlate structural and spectrochemical data with the bonding and reactivity of transition metal nitrosyls. Recent approaches to this problem, based on qualitative molecular orbital considerations,[1] seem able to rationalize much of the data existing for nitrosyl complexes in various coordination geometries.

In the course of previous studies performed in this laboratory a variety of 3d metal complexes with tripod ligands containing group 5 donor atoms have been prepared and characterized.[2] Due to their extreme flexibility, tripod ligands with ethylene bridges are capable of forming metal complexes with various coordination numbers (six,[3] five,[4] four,[5] and intermediate[6]) and different coordination geometries (octahedral,[3] trigonal bipyramidal,[4a] square pyramidal,[4b] square planar,[5a] trigonal pyramidal,[5b] and distorted tetrahedral[6]). It seemed of interest, therefore, to attempt to prepare metal nitrosyl complexes with these ligands as a means of studying the effects on coordination, if any, due to the nitrosyl.

In addition to the neutral complex [Co(NO)(np$_3$)], a variety of metal complexes have been obtained with the general formula [M(NO)L]X (M = Fe, Co, or Ni; L = tris(2-diphenylphosphinoethyl)amine, np$_3$, or tris(2-diphenylarsinoethyl)amine, nas$_3$; X = I, NO$_3$, BF$_4$, BPh$_4$). All of the complexes have been characterized using standard physical methods. The three [M(NO)(np$_3$)]BPh$_4$ derivatives were studied by x-ray diffraction methods. In the nickel case the structure has been completely solved. Structures of the iron and cobalt complexes could not be fully refined owing to the poor quality of the data. Nonetheless, the results obtained do allow significant comparisons to be made between the structures of the three complexes. Preliminary results have been reported elsewhere.[7]

The mononitrosyl complexes have been classified according to a recent approach[1] using the symbol $\{MNO\}^n$ where n is the number of electrons in the highest occupied molecular orbitals bearing a large contribution from the metal atom. This coincides with the number of metal d electrons plus one electron supplied by the NO group, so in the series [M(NO)(np$_3$)]$^+$ n = 8, 9, and 10 for the Fe, Co, and Ni complexes, respectively, which have been investigated by x-ray methods. This avoids the ambiguity of assigning a formal oxidation number to the metal atom in complexes of this type.

Experimental Section

Reagents and Physical Measurements. All solvents were reagent grade and were thoroughly degassed before use. The compounds were prepared in a routine way using degassed solvents under a nitrogen atmosphere; they are air stable. The syntheses of the ligands np$_3$ and nas$_3$ appear elsewhere.[8,9] The physical measurements were executed by previously described methods.[10] The analytical, magnetic, conductivity, and infrared data of the complexes are reported in Table I; Table II lists the electronic spectral data.

Synthesis of Metal Complexes. [Ni(NO)(np$_3$)]X. X = BF$_4$. To a solution of the ligand (2 ml in 60 ml of acetone) Ni(BF$_4$)$_2$·6H$_2$O (2 mmol in 40 ml of ethanol) was added, and the resulting mixture was concentrated. The crystals obtained (corresponding to an average formula of [NiH$_x$(np$_3$)]BF$_4$ (x = 0.06–0.26))[11] were dissolved in 70 ml of dichloromethane and nitrogen oxide was bubbled through for about 20 min until the color turned violet. Dilution with ethanol (30 ml) followed by concentration led to precipitation of black-violet crystals of [Ni(NO)(np$_3$)]BF$_4$.

X = BPh$_4$. This product was obtained by adding 2 mmol of NaBPh$_4$ dissolved in ethanol (25 ml) to the above violet solution. The compound was recrystallized from a THF–ethanol mixture.

X = I. This product was prepared as the tetrafluoroborate derivative, starting from 2 mmol of [NiI(np$_3$)][5b] dissolved in 70 ml of dichloromethane.

X = NO$_3$. After bubbling of NO for 20 min through a stirred suspension of [Ni(NO$_3$)(np$_3$)][11] (1 mmol) in THF (40 ml), a black-violet solution was obtained which on concentration yielded the nitrate derivative. The same compound was also obtained by concentrating a suspension of [Ni(np$_3$)][5b] (2 mmol) in 60 ml of ethanol through which NO had been passed for 30 min. The product was recrystallized from ethanol.

[Ni(NO)(nas$_3$)]X. X = I. The product was obtained by concentrating the solution obtained after bubbling NO for 30 min into a stirred suspension of [NiI(nas$_3$)][12] (2 mmol) in ethanol (60 ml). The compound was recrystallized from acetone–ligroin.

X = BPh$_4$. A solution of NaBPh$_4$ (0.6 mmol) in ethanol (20 ml) was added to a solution of [Ni(NO)(nas$_3$)]I (0.5 mmol) in acetone (40 ml). The complex was obtained by concentration and recrystallized from acetone–ethanol.

[Co(NO)(np$_3$)]. A stream of NO was bubbled into a solution of [CoH(np$_3$)][5b] (2 mmol) in THF (80 ml). Addition of ethanol (40 ml) caused precipitation of the compound which was recrystallized from DMF–ethanol.

[Co(NO)(np$_3$)]BPh$_4$. This was obtained by addition of NaBPh$_4$ (2.5 mmol) in ethanol (40 ml) to a solution of [Co(NO)(np$_3$)] prepared as above, followed by concentration. The green crystals which formed were recrystallized from acetone–ethanol.

[Fe(NO)(np$_3$)]BPh$_4$. Solutions of Fe(BF$_4$)$_2$·6H$_2$O (1 mmol) in ethanol (15 ml) and NaBPh$_4$ (1 mmol) in ethanol (5 ml) were added successively to a solution of the ligand (1 mmol) in THF (20 ml). Nitrogen oxide was bubbled into this solution for ca. 3 min until the color changed from green to violet. Concentration under nitrogen led to precipitation of the product, which was washed with ethanol, petroleum ether, and dried under nitrogen.

Collection and Reduction of X-Ray Intensity Data. Data collection and structure determination have been performed following essentially the same procedure for the three complexes. Details are given for the nickel compound. For the other two complexes only the nature of the experimental difficulties, which prevented an accurate structure determination, is detailed.

[Ni(NO)(np$_3$)]BPh$_4$. The crystal used for data collection was an irregular rectangular prism with dimensions 0.07 × 0.10 × 0.20 mm. The specimen was mounted so that its longest dimension was approximately parallel to the ϕ axis of a Philips computer-controlled PW 1100 diffractometer. Cell constants and the Bravais lattice were

Table I. Analytical and Physical Data for the Complexes

Compd	% calcd				% found				μ_{eff} (293 K), μ_B	Λ_M,[a] cm^2 ohm^{-1} mol^{-1}	μ(NO)[e] cm^{-1}
	C	H	N	M	C	H	N	M			
$[Ni(NO)(np_3)]I$	58.02	4.87	3.22	6.75	58.30	4.97	3.21	6.78	Diam	77	1760
$[Ni(NO)(np_3)]NO_3$	62.71	5.26	5.22	7.30	62.26	5.07	5.43	7.26	Diam	76	1770
$[Ni(NO)(np_3)]BF_4$[b]	60.83	5.11	3.38	7.08	60.79	5.39	3.45	7.11	Diam	82	1775
$[Ni(NO)(np_3)]BPh_4$[c]	74.67	5.89	2.64	5.53	75.25	6.09	2.63	5.42	Diam	49	1755
$[Ni(NO)(nas_3)]I$[d]	50.39	4.23	2.80	5.86	50.53	4.18	2.82	5.94	Diam	60	1760
$[Ni(NO)(nas_3)]BPh_4$	66.42	5.24	2.35	4.92	66.26	5.47	2.30	4.98	Diam	48	1778
$[Co(NO)(np_3)]$	67.92	5.70	3.77	7.94	67.84	5.98	3.87	7.82	Diam		1620
$[Co(NO)(np_3)]BPh_4$	74.65	5.89	2.64	5.55	74.86	6.21	2.66	5.28	1.98	50	1680
$[Fe(NO)(np_3)]BPh_4$	74.87	5.90	2.65	5.27	74.88	5.97	2.58	4.97	Diam	46	1700

[a] Molar conductance of a ca. 10^{-3} M solution in nitroethane at 20 °C. [b] F: calcd, 9.16; found, 9.12. [c] P: calcd, 8.75; found, 8.70. [d] As: calcd, 22.45; found, 22.04. [e] In Nujol mull.

Table II. Absorption Maxima and Extinction Coefficients for the Electronic Spectra of the Complexes

Compd	Absorption max,[a] kK (ϵ_M for soln)
$[Ni(NO)(np_3)]I$	a: 19.7 b: 16.55 sh, 20.2 (930)
$[Ni(NO)(np_3)]NO_3$	a: 16.7 sh, 20.6 b: 16.7 sh, 20.2 (834)
$[Ni(NO)(np_3)]BF_4$	a: 17.1 sh, 20.9 b: 17.1 sh, 20.4 (850)
$[Ni(NO)(np_3)]BPh_4$	a: 16.2 sh, 20.2 b: 16.55 sh, 20.4 (820)
$[Ni(NO)(nas_3)]I$	a: 16.0, 19.1, 26.3 b: 16.4 (628), 18.8 sh, 26.3 (685)
$[Ni(NO)(nas_3)]BPh_4$	a: 16.3 sh, 20.0 b: 16.7 sh, 19.6 (790), 27.3 (712)
$[Co(NO)(np_3)]$	a: 17.0 sh, 20.9 sh b: 17.4 sh, 20.8 sh
$[Co(NO)(np_3)]BPh_4$	a: 6.77, 16.4, 20.8 sh b: 7.15 (51), 17.4 (400)
$[Fe(NO)(np_3)]BPh_4$	a: 20.0 b: 19.6 (1510)

[a] Key: a, solid at room temperature; b, 1,2-dichloroethane solution.

determined using a procedure described elsewhere.[5b] The crystals are triclinic; $P\bar{1}$ was assumed to be the space group and the successful refinement of the structure confirmed this assumption. The unit cell parameters are $a = 18.038$ (8), $b = 16.517$ (7), $c = 10.185$ (5) Å; $\alpha = 86.78$ (8), $\beta = 74.91$ (8), $\gamma = 80.99$ (8)°. The observed density of 1.22 g cm^{-3} (by flotation) agrees with that of 1.219 g cm^{-3} calculated for two molecules per cell.

The intensity data were collected using Mo Kα radiation monochromatized with a flat graphite crystal at a takeoff angle of 4.5°. Reflections for which $2\theta \leq 40°$ were collected using the ω–2θ scan technique over a 2θ interval of 1.2° at a scan speed of 0.12°/s. Stationary-background counts were taken before and after each scan for a time equal to half the scan time. As a check three standard reflections were monitored every 100 min: they showed no significant variations in intensity during data collection.

The total peak counts were corrected for background and the standard deviation $\sigma(I)$ of the resulting intensity I was calculated as described elsewhere[13] using a value of 0.04 for the instability factor K. Of the 5374 reflections collected, 1840 having $I \geq 3\sigma(I)$ were considered observed and included in the following calculations. The value of the linear absorption coefficient is $\mu = 4.63$ cm^{-1} for Mo Kα radiation and no attempt was made to correct for absorption.

$[Co(NO)(np_3)]BPh_4$. Crystals of the compound are isomorphous to those of the nickel analogue; however they provide less suitable material, than those of nickel, for x-ray investigation, due to the exceedingly high mosaic spread. The intensities of diffracted beams show a rapid attenuation with θ. Cell constants, determined by least-squares refinement of the 2θ angles of 29 reflections, are $a = 18.009$ (15), $b = 16.498$ (11), $c = 10.262$ (6) Å; $\alpha = 86.27$ (8), $\beta = 74.52$ (7), $\gamma = 80.43$ (8)°. The observed density of 1.21 g cm^{-3} (by flotation) agrees with that of 1.217 g cm^{-3} calculated for two molecules per cell.

Two sets of data were collected using two crystals of very different size with dimensions (a) 0.012 × 0.034 × 0.250 and (b) 0.050 × 0.100 × 0.600 mm, along the [100], [010], and [001] directions, in that order. Both crystals were mounted along their c axes for data collection. A total of 6316 independent reflections were collected to $2\theta \leq 44°$, yielding only (a) 876 and (b) 796 reflections with $I \geq 2.5(I)$ which were subsequently used for two independent sets of calculations. The fact that the number of observed reflections does not increase with increasing volume of the crystal may be attributed to the poor quality of the reflecting material. The intensities of three standard reflections showed no systematic trend during data collections. The linear absorption coefficient is 4.17 cm^{-1} for Mo Kα radiation and no correction for absorption was applied.

$[Fe(NO)(np_3)]BPh_4$. Well-developed blue crystals occur as rectangular prisms. The intensities of reflections decrease rapidly with θ, as for the cobalt analogue. In addition, Weissenberg photographs show some streaks due to scattered radiation, along directions parallel to [100]*. This may be caused by a degree of disordering, essentially restricted to planes parallel to (100) (see below). Systematic absences ($h0l$) and ($0kl$), $l = 2n + 1$, ($hk0$), $h + k = 2n + 1$, ($h00$), ($0k0$), and ($00l$), h, k, and $l = 2n + 1$, establish the space group as the orthorhombic *Pccn*. The cell constants are $a = 33.35$ (8), $b = 18.54$ (2), $c = 18.47$ (2) Å. The value of the density, calculated for eight molecules in the unit cell is 1.23 g cm^{-3}, which agrees with that of 1.23 g cm^{-3} measured by flotation; μ(Mo Kα) = 3.86 cm^{-1}. The intensities of three standard reflections revealed no systematic trends during data collection. Of the 5178 reflections examined, having $2\theta \leq 40°$, only 1021 had $I \geq 3\sigma(I)$ and were used for structure determination.

Solution and Refinement of the Structures. All calculations were carried out using the XRY72 crystallographic system[14] and the ORTEP program,[15] adapted to the University of Florence CII 10070 computer. The atomic scattering factors calculated by Cromer and Waber[16] were used for all nonhydrogen atoms; those calculated by Stewart, Davidson, and Simpson[17] were used for hydrogen.

$[Ni(NO)(np_3)]BPh_4$. The position of the nickel atom was determined from a three-dimensional Patterson map. Successive three-dimensional Fourier syntheses showed the positions of all the nonhydrogen atoms. Full-matrix least-squares refinement was then undertaken: the function minimized was $\sum w(|F_o| - |F_c|)^2$ and the weights w were set to unity at this stage. Two cycles of isotropic refinement followed by two cycles using anisotropic thermal parameters for the nickel, phosphorus, oxygen, and nitrogen atoms and isotropic parameters for the other atoms reduced the conventional R factor to 0.086. The hydrogen atoms were then introduced in calculated position (C–H = 1.0 Å), with temperature factors equal to those of their carbon atoms. Their parameters were not refined in subsequent calculations but were adjusted after each cycle to match the shifts undergone by parameters of carbon atoms. After several cycles of refinement, convergence was attained, the final values of the discrepancy indices R and R_w being 0.068 and 0.072, respectively; $R_w = [\sum w(|F_o| - |F_c|)^2/\sum wF_o^2]^{1/2}$. In the final refinement weights w were taken as $1/\sigma(F_o)$. The real and imaginary corrections[18] for anomalous dispersion for the nickel and phosphorus atoms were applied. The standard deviation of an observation of unit weight is 1.38.

$[Co(NO)(np_3)]BPh_4$. The structure was solved by the heavy-atom method independently from that of the isomorphous nickel compound. Least-squares refinement was separately performed using the two sets of data, from crystals (a) and (b) (see above); derived parameters essentially agree, within 3σ. Results are reported for data collected with crystal (b), which gave slightly lower R and σ values. The final

Table III. $[Ni(NO)(np_3)]BPh_4$ Positional Parameters and Isotropic Thermal Parameters, with Estimated Standard Deviations in Parentheses

Atom	*x/a*	*y/b*	*z/c*	10^2U, Å^2
Ni	0.1632 (1)	0.2685 (1)	0.2915 (2)	
P(1)	0.1870 (3)	0.3226 (3)	0.0763 (5)	
P(2)	0.1873 (3)	0.1285 (3)	0.2700 (5)	
P(3)	0.2621 (3)	0.2958 (3)	0.3786 (5)	
O	0.018 (1)	0.345 (2)	0.412 (3)	
N(1)	0.335 (1)	0.203 (1)	0.107 (1)	
N(2)	0.079 (1)	0.309 (1)	0.375 (2)	
C(1)	0.338 (1)	0.246 (1)	−0.023 (2)	5.2 (5)
C(2)	0.260 (1)	0.263 (1)	−0.056 (2)	6.2 (6)
C(3)	0.335 (1)	0.117 (1)	0.100 (2)	5.0 (5)
C(4)	0.288 (1)	0.082 (1)	0.229 (2)	5.3 (5)
C(5)	0.388 (1)	0.225 (1)	0.180 (2)	5.5 (5)
C(6)	0.355 (1)	0.304 (1)	0.255 (2)	5.1 (5)
C(7)	0.216 (1)	0.424 (1)	0.062 (2)	4.0 (5)
C(8)	0.196 (1)	0.474 (1)	0.174 (2)	6.3 (6)
C(9)	0.217 (1)	0.551 (1)	0.170 (2)	7.2 (6)
C(10)	0.259 (1)	0.576 (1)	0.053 (2)	8.6 (7)
C(11)	0.279 (1)	0.534 (1)	−0.061 (2)	10.2 (8)
C(12)	0.257 (1)	0.454 (1)	−0.057 (2)	7.9 (7)
C(13)	0.104 (1)	0.338 (1)	0.006 (2)	5.1 (5)
C(14)	0.099 (1)	0.297 (1)	−0.103 (2)	7.9 (7)
C(15)	0.031 (1)	0.307 (1)	−0.151 (2)	9.4 (7)
C(16)	−0.033 (1)	0.358 (1)	−0.087 (2)	10.0 (8)
C(17)	−0.031 (1)	0.400 (1)	0.018 (2)	11.5 (9)
C(18)	0.038 (1)	0.388 (1)	0.070 (2)	8.3 (7)
C(19)	0.140 (1)	0.071 (1)	0.420 (2)	5.4 (5)
C(20)	0.171 (1)	−0.005 (1)	0.450 (2)	7.8 (7)
C(21)	0.131 (1)	−0.050 (1)	0.560 (2)	8.2 (7)
C(22)	0.060 (1)	−0.018 (1)	0.637 (2)	7.8 (7)
C(23)	0.029 (1)	0.060 (1)	0.609 (2)	7.9 (7)
C(24)	0.068 (1)	0.103 (1)	0.498 (2)	6.2 (6)
C(25)	0.150 (1)	0.088 (1)	0.137 (2)	6.0 (6)
C(26)	0.183 (1)	0.014 (1)	0.079 (2)	10.6 (8)
C(27)	0.149 (1)	−0.013 (1)	−0.021 (2)	12.2 (9)
C(28)	0.090 (1)	0.035 (2)	−0.046 (3)	11.9 (9)
C(29)	0.054 (1)	0.104 (1)	0.008 (2)	10.5 (8)
C(30)	0.087 (1)	0.135 (1)	0.109 (2)	9.2 (7)
C(31)	0.240 (1)	0.390 (1)	0.472 (2)	5.4 (5)
C(32)	0.287 (1)	0.448 (1)	0.458 (2)	8.1 (7)
C(33)	0.265 (1)	0.519 (1)	0.540 (2)	10.3 (8)
C(34)	0.197 (1)	0.530 (1)	0.631 (2)	11.0 (8)
C(35)	0.146 (1)	0.476 (2)	0.647 (3)	13.1 (9)
C(36)	0.170 (1)	0.403 (1)	0.570 (2)	10.9 (8)
C(37)	0.288 (1)	0.221 (1)	0.505 (2)	4.3 (5)
C(38)	0.361 (1)	0.206 (1)	0.526 (2)	4.9 (5)
C(39)	0.377 (1)	0.146 (1)	0.623 (2)	7.3 (6)
C(40)	0.321 (1)	0.106 (1)	0.696 (2)	6.6 (6)
C(41)	0.248 (1)	0.119 (1)	0.680 (2)	6.7 (6)
C(42)	0.231 (1)	0.178 (1)	0.584 (2)	5.0 (5)
C(43)	0.437 (1)	0.692 (1)	0.237 (2)	5.7 (6)
C(44)	0.501 (1)	0.696 (1)	0.290 (2)	6.7 (6)
C(45)	0.547 (1)	0.629 (1)	0.333 (2)	9.9 (8)
C(46)	0.529 (1)	0.551 (1)	0.325 (2)	9.1 (7)
C(47)	0.468 (1)	0.543 (1)	0.276 (2)	9.1 (7)
C(48)	0.421 (1)	0.612 (1)	0.229 (2)	8.0 (7)
C(49)	0.398 (1)	0.772 (1)	0.019 (2)	6.1 (6)
C(50)	0.382 (1)	0.843 (1)	−0.055 (2)	7.1 (6)
C(51)	0.389 (1)	0.844 (1)	−0.201 (2)	9.6 (8)
C(52)	0.416 (1)	0.773 (2)	−0.266 (2)	10.8 (8)
C(53)	0.433 (1)	0.702 (1)	−0.201 (3)	9.9 (8)
C(54)	0.427 (1)	0.701 (1)	−0.063 (2)	8.3 (7)
C(55)	0.289 (1)	0.764 (1)	0.253 (2)	6.7 (6)
C(56)	0.235 (1)	0.790 (1)	0.177 (2)	9.6 (8)
C(57)	0.153 (1)	0.786 (1)	0.232 (3)	11.7 (9)
C(58)	0.133 (1)	0.757 (1)	0.360 (3)	11.7 (9)
C(59)	0.180 (1)	0.732 (1)	0.434 (2)	9.7 (8)
C(60)	0.264 (1)	0.736 (1)	0.385 (2)	10.0 (8)
C(61)	0.407 (1)	0.854 (1)	0.233 (2)	5.2 (5)
C(62)	0.376 (1)	0.883 (1)	0.370 (2)	5.9 (6)
C(63)	0.400 (1)	0.947 (1)	0.418 (2)	7.2 (6)
C(64)	0.452 (1)	0.989 (1)	0.336 (2)	6.0 (6)
C(65)	0.487 (1)	0.966 (1)	0.203 (2)	6.1 (6)
C(66)	0.461 (1)	0.899 (1)	0.156 (2)	5.4 (5)
B	0.384 (1)	0.769 (1)	0.180 (2)	5.5 (6)

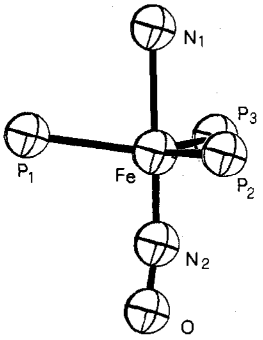

Figure 1. Perspective view of the coordination polyhedron of the $[Fe(NO)(np_3)]^+$ cation (ORTEP diagram showing 50% probability ellipsoids).

R and R_w values are 0.142 and 0.145, respectively. Weights were taken as $1/\sigma(F_o)$. No correction for anomalous dispersion was applied. Hydrogen atoms were not located or introduced in calculated position. A final ΔF synthesis showed a number of peaks having heights ca. one-third that of a carbon atom, measured from a ΔF Fourier calculated without contribution from that carbon atom. The peaks were randomly distributed throughout the map and could not be assigned any significance. ΔF values do not exhibit any significant trend. The high final *R* and σ values should be attributed to the poor quality of the data, consisting of a small number of low-intensity and low-angle reflections, for both crystals. That the structure determination is essentially correct, in spite of the above values of the indicators, is proved by the agreement between refinements performed with the two sets of data and by overall agreement with the structure of the isomorphous nickel compound.

Listings of the observed and calculated structure factors for the nickel and cobalt compounds are available (supplementary material). The final positional and thermal parameters are listed in Tables III–V.

$[Fe(NO)(np_3)]BPh_4$. The important features of the structure were determined by the heavy-atom procedure. Atoms in the coordination polyhedron and carbon atoms close to these were readily located. Using known geometry of the phenyl rings to solve few ambiguities, all carbon atom positions in the cation could be assigned from Fourier syntheses. Disordering was found to affect essentially three phenyl groups in the anion. These occupy a volume with dimensions ca. 3 × 7 × 7 Å^3, along the [100], [010], and [001] directions, respectively. The BPh_3 moiety is disordered about a direction close to the crystallographic [100]. The positions of the boron atom and of carbon atoms belonging to the fourth phenyl group of the anion could be determined. Parameters for these atoms and for those of the cation were refined by a set of isotropic full-matrix least squares, which yielded dimensions within the organic part of the structure in reasonable agreement with expected values. *R* was 0.199 at this point. Examination of a ΔF Fourier did not suggest improvements to the model. No unreasonably short nonbonded distances exist between atoms refined.

In spite of the difficulties posed by disorder, we believe that the results for the gross features of the coordination in this complex may be accepted with confidence. In fact the environment of the metal atom is not directly involved in the disorder: the large values of errors on the atomic positions in the polyhedron are caused by the overall poor quality of the data. Even though some details of the structure have not been unraveled, we nevertheless think that we have achieved our goal which was determining the geometry of coordination in this compound.[19]

The important atomic positions are listed in Table VI. We do not deem it is worthwhile to report detailed results, in view of the disorder existing in the structure of this compound.

Description of the Structures

The structures of the three complexes consist of $[M(NO)(np_3)]^+$ cations and BPh_4^- anions. Figure 1 shows the coordination polyhedron for the iron complex (**1**) and Figure 2 shows perspective views of the cations in the cobalt (**2**) and nickel (**3**) complexes. Values of important bond distances and angles are reported in Tables VII and VIII.

In the iron complex the metal atom is surrounded by the four donor atoms of the tripod ligand and by the nitrosyl nitrogen atom in a trigonal-bipyramidal arrangement. The

Table IV. $[Ni(NO)(np_3)]BPh_4$ Anisotropic Thermal[a] Parameters ($\times 10^2$), with Esd's in Parentheses

Atom	U_{11}	U_{22}	U_{33}	U_{12}	U_{13}	U_{23}
Ni	3.8 (2)	4.3 (2)	4.9 (2)	−0.1 (1)	−0.7 (1)	0.1 (1)
P(1)	4.4 (4)	3.8 (3)	4.8 (4)	−0.6 (3)	−1.3 (3)	−0.3 (3)
P(2)	3.8 (3)	4.2 (3)	4.7 (4)	−0.6 (3)	−1.6 (3)	0.2 (3)
P(3)	4.3 (3)	4.6 (3)	4.2 (4)	−0.8 (3)	−0.8 (3)	−0.7 (3)
O	11.0 (1.8)	27.5 (3.0)	33.7 (3.4)	9.8 (1.9)	9.2 (2.0)	10.4 (2.5)
N(1)	4.2 (9)	4.4 (9)	3.9 (1.0)	−0.3 (7)	−1.5 (8)	−0.7 (7)
N(2)	3.6 (1.2)	10.1 (1.5)	12.6 (1.7)	1.9 (1.1)	2.0 (1.2)	4.0 (1.3)

[a] The form of the anisotropic thermal factor is $\exp[-2\pi^2(U_{11}h^2a^{*2} + U_{22}k^2b^{*2} + U_{33}l^2c^{*2} + 2U_{12}hka^*b^* \cos\gamma^* + 2U_{13}hla^*c^* \cos\beta^* + 2U_{23}klb^*c^* \cos\alpha^*)]$.

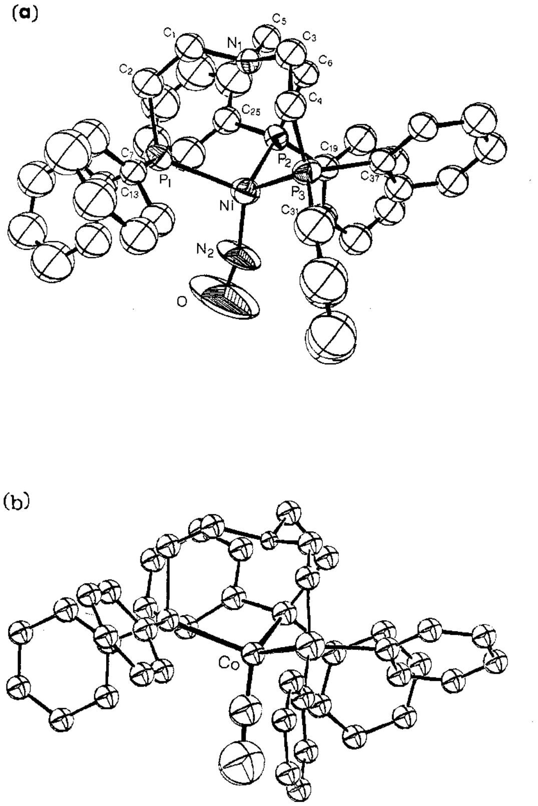

Figure 2. ORTEP perspective views of the $[Ni(NO)(np_3)]^+$ cation (a) and of the $[Co(NO)(np_3)]^+$ cation (b). All carbon atoms in (b) have been assigned an identical value for the temperature factor; labeling in (b) is as in (a).

cobalt and nickel complexes, in contrast, are both tetrahedrally coordinated with the metal atom bonded to the NO nitrogen and to the three phosphorus atoms of the ligand. In the last two complexes the nitrogen atom of the tripod ligand is separated from the metal atom by distances far in excess of normal bond lengths (Table VII) and is therefore regarded as noncoordinating.

Differences in the coordination between the three complexes are clearly shown by a comparison between mean values of the P–M–N(NO) and P–M–P angles (averaging over chemically equivalent sets of angles should be allowed to establish crude comparisons, in view of the large difference existing even between the two tetrahedral complexes). Values of these angles for the complexes **1**, **2**, and **3**, respectively, are P–M–N(NO) = 94.4, 107.2, and 113.5°, P–M–P = 119.1, 111.7, and 105.1°. The metal atom deviates from the plane of the three phosphorus atoms by 0.17, 0.69, and 0.92 Å, for the complexes in the above order.

It is worth commenting here that the "tetrahedral distortion" which is larger for the nickel complex (**3**) as compared to the cobalt isomorph (**2**) (and which in the nickel case is accompanied by straining of the ligand chain, C–N–C = 114.0 (0.7)° average) has been found previously, though to a less marked extent, in high-spin cobalt(II) complexes[6] (e.g., Cl–Co–P = 104.6° and P–Co–P = 113.8°, average values in $[CoCl(np_3)]PF_6$[6a]). Clearly, the fact that np_3 does not impose rigid requirements on stereochemistry in the present structures is in line with the coordination characteristics associated with this ligand in related transition metal complexes.[3–6] The 167.7 (2.1)° value of the M–N–O angle for the nickel complex falls in the range of the linear MNO group, according to current views.[1] Essentially the same type of geometry may be assigned to the MNO group in the other two complexes (164 (7)° (**1**) and 165 (7)° (**2**)) although the large values of the standard deviations make conclusions less certain in the latter cases. However, it should be noted in this connection, that a linear MNO group in the axial position has been found for the related iron complex of ref 19.

To our knowledge, complex **1** and the complex $[Fe(NO)(pp_3)]BPh_4$[19] are the first examples of $\{FeNO\}^8$ complexes so far reported. Trigonal-bipyramidal coordination has been found in two other $\{MNO\}^8$ complexes[20] formed by metals different from iron. No previous report of a $\{MNO\}^9$ complex, having a coordination geometry similar to that found in the present cobalt complex, exists. The geometry in **3** is close to that found in the $[Ni(P(OCH_2)_3CCH_3)_3NO]^+$ cation,[21] where four monodentate ligands are present, and may be compared to that in the $[Ni(tep)NO]^+$ cation[22] (tep = $CH_3C(CH_2PEt_2)_3$), where, however, limitations are imposed by the nature of the tep ligand.

Bond distances and angles not involving the metal atom are normal in complex **3** and are in the normal range also in complexes **1** and **2**, considering the large values of σ's on parameters in the latter structures. There are no unusually short contact distances.

Results and Discussion

Nickel Complexes, $[Ni(NO)L]X$ (L = np_3, nas_3; X = I, NO_3, BF_4, BPh_4). These black-violet complexes are air stable, are soluble in common organic solvents, and behave as 1:1 electrolytes. The complexes are all diamagnetic and exhibit very similar solution and reflectance spectra, which consist of a main absorption in the region 16–21 kK, split into two components (Table II, Figure 3). When L = nas_3, the spectra differ slightly from this pattern by the appearance of a shoulder on the low-energy side of the charge-transfer band. The NO group stretching frequencies (Table I) fall in the range 1755–1775 cm^{-1}; these are compared below with corresponding values for complexes of the other metals. All of these nickel complexes may be assigned the tetrahedral coordination geometry, determined for complex **3**, in view of the similarity of their properties.

$[Co(NO)(np_3)]$. This diamagnetic brown compound is stable in air and insoluble in nitroethane. The charge-transfer bands in this neutral complex fall at lower frequencies than in the previous isoelectronic nickel complexes, thus masking ligand field transitions. However, two shoulders may be observed (Table II) in the positions of the two components of the band which is present in the spectra of the nickel complexes. These results are consistent with a tetrahedral geometry of coor-

Table V. $[Co(NO)(np_3)]BPh_4$ Positional and Thermal Parameters, with (Esd's in Parentheses)

Atom	x/a	y/b	z/c	$10^2 U$, Å^2
CO	0.1764 (6)	0.2657 (6)	0.2752 (10)	4.3 (4)
P(1)	0.1864 (13)	0.3293 (14)	0.0756 (23)	8.4 (9)
P(2)	0.1869 (13)	0.1237 (13)	0.2756 (22)	8.4 (9)
P(3)	0.2686 (13)	0.2925 (14)	0.3855 (23)	9.4 (9)
O	0.011 (5)	0.321 (5)	0.408 (9)	31.9 (5.5)
N(1)	0.330 (3)	0.206 (3)	0.100 (5)	3.7 (1.7)
N(2)	0.077 (4)	0.308 (4)	0.367 (6)	9.3 (2.5)
C(1)	0.349 (4)	0.258 (4)	−0.010 (8)	8.0 (2.7)
C(2)	0.280 (4)	0.265 (4)	−0.060 (7)	10.8 (3.1)
C(3)	0.335 (3)	0.115 (4)	0.117 (6)	2.9 (1.9)
C(4)	0.284 (3)	0.077 (3)	0.216 (6)	4.6 (2.2)
C(5)	0.399 (4)	0.212 (4)	0.186 (7)	9.5 (2.7)
C(6)	0.366 (4)	0.307 (4)	0.254 (7)	8.8 (2.7)
C(7)	0.217 (3)	0.422 (4)	0.043 (6)	6.7 (2.4)
C(8)	0.205 (4)	0.470 (4)	0.192 (8)	10.6 (3.0)
C(9)	0.214 (4)	0.554 (4)	0.156 (7)	8.1 (2.6)
C(10)	0.266 (4)	0.586 (5)	0.053 (8)	12.9 (3.6)
C(11)	0.277 (6)	0.542 (6)	−0.065 (11)	20.2 (5.1)
C(12)	0.256 (4)	0.465 (4)	−0.059 (7)	9.3 (2.9)
C(13)	0.111 (5)	0.354 (6)	−0.014 (11)	16.7 (4.2)
C(14)	0.035 (6)	0.386 (5)	0.075 (8)	11.9 (3.4)
C(15)	−0.028 (5)	0.404 (5)	0.030 (10)	13.4 (3.8)
C(16)	−0.040 (5)	0.359 (5)	−0.097 (9)	12.1 (3.4)
C(17)	0.034 (6)	0.313 (5)	−0.160 (9)	13.5 (3.8)
C(18)	0.098 (5)	0.310 (5)	−0.128 (9)	11.1 (3.3)
C(19)	0.132 (4)	0.074 (5)	0.426 (7)	7.6 (2.6)
C(20)	0.061 (4)	0.112 (4)	0.502 (8)	7.9 (2.6)
C(21)	0.028 (4)	0.060 (5)	0.610 (7)	6.5 (2.5)
C(22)	0.061 (4)	−0.013 (5)	0.625 (7)	8.3 (2.8)
C(23)	0.142 (5)	−0.049 (5)	0.572 (9)	12.0 (3.4)
C(24)	0.172 (3)	−0.004 (4)	0.456 (7)	5.4 (2.4)
C(25)	0.139 (5)	0.096 (6)	0.129 (9)	15.1 (4.8)
C(26)	0.091 (6)	0.144 (6)	0.096 (11)	17.9 (4.8)
C(27)	0.043 (6)	0.127 (7)	0.010 (12)	22.4 (5.4)
C(28)	0.077 (5)	0.051 (5)	−0.044 (8)	14.9 (3.8)
C(29)	0.134 (5)	−0.011 (5)	−0.023 (8)	13.7 (3.6)
C(30)	0.168 (4)	−0.007 (4)	0.090 (7)	7.7 (2.6)
C(31)	0.230 (6)	0.406 (5)	0.496 (8)	11.9 (3.3)
C(32)	0.148 (7)	0.407 (7)	0.598 (11)	21.3 (5.1)
C(33)	0.132 (6)	0.500 (7)	0.602 (10)	17.0 (4.4)
C(34)	0.191 (6)	0.540 (5)	0.608 (8)	11.2 (3.4)
C(35)	0.283 (7)	0.530 (7)	0.515 (11)	22.6 (5.1)
C(36)	0.295 (5)	0.448 (5)	0.456 (8)	12.5 (3.4)
C(37)	0.286 (4)	0.225 (4)	0.508 (6)	5.2 (2.3)
C(38)	0.222 (3)	0.175 (4)	0.587 (6)	3.1 (1.9)
C(39)	0.247 (4)	0.111 (4)	0.679 (7)	7.8 (2.8)
C(40)	0.313 (4)	0.097 (4)	0.705 (6)	4.3 (2.2)
C(41)	0.370 (3)	0.142 (3)	0.646 (6)	2.9 (1.9)
C(42)	0.355 (3)	0.203 (3)	0.539 (5)	1.5 (1.8)
C(43)	0.444 (4)	0.689 (4)	0.236 (6)	7.1 (2.5)
C(44)	0.503 (4)	0.702 (4)	0.282 (6)	5.1 (2.3)
C(45)	0.554 (3)	0.623 (4)	0.330 (6)	4.8 (2.2)
C(46)	0.524 (4)	0.541 (4)	0.331 (6)	6.7 (2.5)
C(47)	0.462 (4)	0.546 (4)	0.271 (7)	7.3 (2.6)
C(48)	0.412 (4)	0.612 (4)	0.236 (7)	9.4 (2.8)
C(49)	0.393 (4)	0.781 (5)	0.006 (7)	8.7 (3.0)
C(50)	0.434 (4)	0.697 (4)	−0.061 (8)	9.6 (3.0)
C(51)	0.432 (4)	0.712 (5)	−0.214 (8)	7.2 (2.8)
C(52)	0.411 (5)	0.780 (7)	−0.243 (9)	13.5 (3.9)
C(53)	0.388 (7)	0.866 (8)	−0.215 (15)	26.6 (6.6)
C(54)	0.371 (5)	0.847 (7)	−0.064 (12)	17.0 (4.5)
C(55)	0.284 (4)	0.766 (4)	0.262 (9)	8.3 (2.7)
C(56)	0.274 (5)	0.733 (5)	0.390 (10)	12.1 (3.4)
C(57)	0.185 (5)	0.725 (5)	0.460 (8)	10.7 (3.1)
C(58)	0.136 (4)	0.755 (5)	0.356 (9)	9.4 (3.2)
C(59)	0.154 (5)	0.785 (5)	0.238 (9)	10.1 (3.2)
C(60)	0.237 (5)	0.798 (4)	0.160 (7)	7.7 (2.8)
C(61)	0.407 (4)	0.862 (4)	0.236 (9)	8.6 (2.8)
C(62)	0.371 (5)	0.886 (6)	0.380 (11)	17.1 (4.4)
C(63)	0.402 (5)	0.956 (5)	0.408 (8)	11.7 (3.4)
C(64)	0.462 (5)	0.989 (5)	0.325 (11)	13.1 (3.7)
C(65)	0.492 (4)	0.975 (5)	0.182 (9)	10.7 (3.2)
C(66)	0.463 (4)	0.904 (4)	0.152 (7)	6.6 (2.5)
B	0.380 (4)	0.767 (4)	0.197 (7)	5.3 (2.7)

Table VI. $[Fe(NO)(np_3)]BPh_4$ Positional and Thermal Parameters of Atoms in the Coordination Polyhedron, with Esd's in Parentheses

Atom	x/a	y/b	z/c	$10^2 U$, Å^2
Fe	0.3950 (5)	0.4762 (9)	0.0727 (9)	3.7 (5)
P(1)	0.4048 (9)	0.3703 (17)	0.0158 (18)	4.3 (1.0)
P(2)	0.3894 (8)	0.4895 (14)	0.1924 (14)	3.6 (9)
P(3)	0.3749 (9)	0.5663 (19)	−0.0013 (20)	5.4 (1.1)
O	0.474 (2)	0.511 (3)	0.079 (3)	4.4 (1.7)
N(1)	0.334 (3)	0.440 (5)	0.067 (5)	5.6 (2.7)
N(2)	0.440 (2)	0.505 (2)	0.071 (4)	3.5 (2.2)

Table VII. Bond Lengths (Å) and Angles (deg) within the Coordination Polyhedra (Esd's in Parentheses)

	M = Fe	M = Co	M = Ni
	Lengths		
M–P(1)	2.24 (4)	2.22 (2)	2.280 (5)
M–P(2)	2.22 (3)	2.32 (2)	2.297 (5)
M–P(3)	2.25 (4)	2.36 (3)	2.302 (6)
M–N(1)	2.15 (8)	2.92 (4)	3.23 (1)
M–N(2)	1.60 (7)	1.83 (6)	1.59 (2)
N(2)–O	1.19 (9)	1.14 (10)	1.14 (3)
	Angles		
P(1)–M–P(2)	124.9 (1.3)	116.1 (9)	106.5 (2)
P(1)–M–P(3)	114.0 (1.4)	113.6 (9)	105.7 (2)
P(2)–M–P(3)	119.3 (1.3)	105.5 (9)	103.1 (2)
P(1)–M–N(2)	98.0 (2.7)	101.5 (2.0)	108.5 (7)
P(2)–M–N(2)	93.8 (2.9)	108.5 (2.0)	118.4 (7)
P(3)–M–N(2)	91.4 (2.8)	111.7 (2.4)	113.6 (8)
P(1)–M–N(1)	81.6 (2.5)	72.0 (1.2)	66.7 (5)
P(2)–M–N(1)	89.8 (2.6)	73.7 (1.2)	66.8 (5)
P(3)–M–N(1)	85.0 (2.5)	73.2 (1.3)	65.8 (5)
N(1)–M–N(2)	175.8 (3.8)	173.3 (2.3)	174.3 (7)
M–N(2)–O	164 (7)	165 (7)	167.7 (2.1)

Table VIII. $[Ni(NO)(np_3)]BPh_4$ Selected Bond Lengths (Å) and Angles (deg) in the Ligand (Esd's in Parentheses)

	Lengths		
P(1)–C(2)	1.83 (2)	P(3)–C(37)	1.83 (2)
P(1)–C(7)	1.81 (2)	N(1)–C(1)	1.46 (2)
P(1)–C(13)	1.80 (2)	N(1)–C(3)	1.43 (2)
P(2)–C(4)	1.81 (2)	N(1)–C(5)	1.45 (2)
P(2)–C(19)	1.84 (2)	C(1)–C(2)	1.52 (3)
P(2)–C(25)	1.86 (2)	C(3)–C(4)	1.51 (2)
P(3)–C(6)	1.84 (2)	C(5)–C(6)	1.51 (2)
P(3)–C(31)	1.80 (2)		
	Angles		
Ni–P(1)–C(2)	117.1 (6)	C(6)–P(3)–C(31)	104.1 (8)
Ni–P(1)–C(7)	114.2 (6)	C(6)–P(3)–C(37)	104.1 (7)
Ni–P(1)–C(13)	114.1 (6)	C(31)–P(3)–C(37)	101.6 (8)
C(2)–P(1)–C(7)	105.1 (7)	Ni–N(1)–C(1)	104.0 (6)
C(2)–P(1)–C(13)	101.7 (9)	Ni–N(1)–C(3)	103.6 (6)
C(7)–P(1)–C(13)	102.9 (8)	Ni–N(1)–C(5)	105.4 (6)
Ni–P(2)–C(4)	116.7 (6)	C(1)–N(1)–C(3)	112.9 (1.3)
Ni–P(2)–C(19)	114.9 (6)	C(1)–N(1)–C(5)	114.6 (1.3)
Ni–P(2)–C(25)	115.0 (6)	C(3)–N(1)–C(5)	114.4 (1.3)
C(4)–P(2)–C(19)	105.1 (8)	N(1)–C(1)–C(2)	112.6 (1.3)
C(4)–P(2)–C(25)	103.0 (8)	N(1)–C(3)–C(4)	112.5 (1.3)
C(19)–P(2)–C(25)	100.2 (9)	N(1)–C(5)–C(6)	111.0 (1.3)
Ni–P(3)–C(6)	116.4 (6)	C(1)–C(2)–P(1)	111.9 (1.3)
Ni–P(3)–C(31)	114.1 (6)	C(3)–C(4)–P(2)	112.5 (1.2)
Ni–P(3)–C(37)	114.7 (6)	C(5)–C(6)–P(3)	111.1 (1.2)

dination, as that ascertained for complex **3**.

$[Co(NO)(np_3)]BPh_4$. This green air-stable compound is soluble in common organic solvents and behaves as a 1:1 electrolyte. The magnetic moment of 1.98 μ_B is close to the spin-only value for one unpaired electron. The absorption spectrum shows an intense band at ca. 17.4 kK and a weaker one at 7.1 kK. In the reflectance spectrum (Figure 3, Table II) a shoulder is observed at high frequencies. As this is well-resolved from the main ligand field excitation, there is no close resemblance to the nickel spectra.

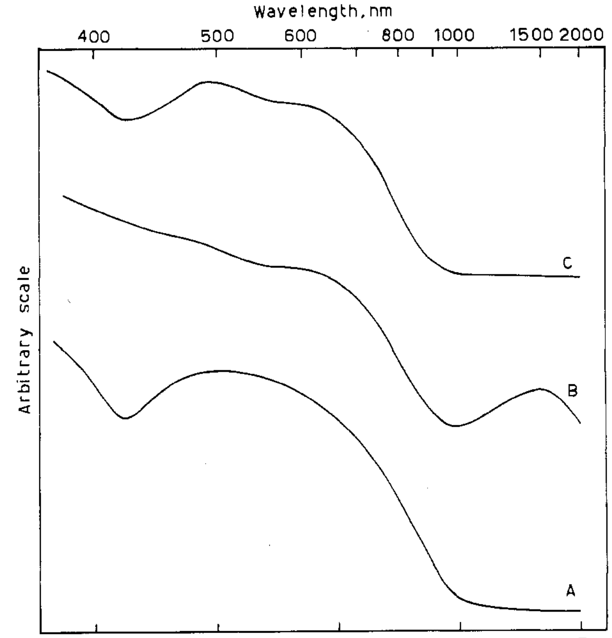

Figure 3. Reflectance spectra of $[Fe(NO)(np_3)]BPh_4$ (A), $[Co(NO)(np_3)]BPh_4$ (B), and $[Ni(NO)(np_3)]BPh_4$ (C).

$[Fe(NO)(np_3)]BPh_4$. This blue-violet air-stable compound is soluble in common solvents and is a 1:1 electrolyte. It is diamagnetic. There is one intense band in the visible–uv part of the spectrum (Figure 3).

The structures and principal physical properties of all these nitrosyl complexes may be rationalized in terms of a simple molecular orbital approach. Essentially the reasoning is that the d-orbital manifold, being split in a field of appropriate symmetry, interacts strongly with the nitric oxide orbitals (σ(NO) and π^*(NO)) of comparable energy.[1] Interactions between metal and other ligand orbitals are treated as a minor perturbation and are not explicitly considered in this scheme. This approach has been successfully applied to nitrosyl complexes with various coordination geometries[1] and is here extended to C_{3v} geometry, which is the idealized arrangement present in all complexes investigated, with the NO group occupying an axial position.

Figure 4a shows schematically the formation of molecular orbitals via interaction of the metal d orbitals with the nitrogen lone pair σ(NO) and the degenerate antibonding orbitals π^*(NO) on the nitric oxide ligand. It has been established[1] that the metal and the π^*(NO) orbitals have comparable energy. The relative positions of these two orbital sets have important consequences insofar as the interpretation of experimental results is concerned. However, since this ordering is sensitive to such factors as the nature and oxidation state of the metal atom, the nature of the donor set, and the geometry of coordination, it cannot be safely predicted for individual complexes. In C_{3v} symmetry, for example, alternative arrangements of the uppermost 3e and $2a_1$ levels may arise (Figure 4b and c) depending on the relative importance of the above factors. The $1a_1$ orbital, included in Figure 4a, has been omitted from the other schemes in Figure 4, being not relevant to the following considerations. Assigning all metal d electrons plus one electron contributed by the π^*(NO) orbitals to the levels in Figure 4c, the following configurations arise: for the $[Ni(NO)(np_3)]^+$ and the $[Co(NO)(np_3)]$ complexes, which are all $\{MNO\}^{10}$ species, the $(1e)^4(2e)^4(2a_1)^2$ configuration; for the $\{MNO\}^9$ $[Co(NO)(np_3)]BPh_4$ complex, $(1e)^4(2e)^4 2a_1$; and for the $\{MNO\}^8$ iron complex, $(1e)^4(2e)^4$. The diamagnetic behavior is thus anticipated for all even-electron complexes and in addition a μ_{eff} close to the spin-only value for $[Co(NO)(np_3)]BPh_4$ is expected; in fact the orbital singlet ground state of the latter is far removed from excited states (see below, discussion of the spectra). Recourse to the level scheme of Figure 4b, on the other hand, does not account for the experimental results.

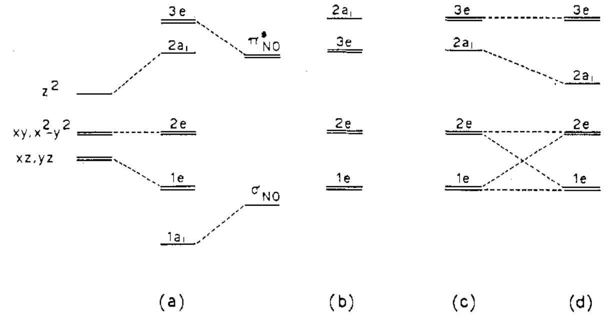

Figure 4. Schematic molecular orbital diagrams: (a) interaction between metal d orbitals and nitric oxide orbitals, in C_{3v} symmetry (see text); (b) energy level scheme, assuming $E(3d) \simeq E(\pi^*(NO))$; (c) $E(3d) < E(\pi^*(NO))$; (d) effect of tetrahedral distortion on the energy levels shown in (c).

The level ordering of Figure 4c, which will be adopted from now on, allows the geometries of the complexes to be rationalized. The trends connecting the schemes of Figure 4c and d illustrate the changes that occur in the course of the tetrahedral distortion from trigonal bipyramidal geometry: the $2a_1$ level becomes considerably stabilized, whereas the energy of the lower lying e levels, which mix together, is substantially unaffected. This view is supported by EHMO calculations[6b] on series of complexes having the same coordination geometry. Therefore the tetrahedral distortion, which preserves C_{3v} symmetry, is dictated by stabilization of the "frontier orbital" $2a_1$, which is the highest occupied orbital in the cobalt and nickel complexes. The extent of the distortion should depend on the population of that orbital; in fact it is found to be larger for the nickel than for the cobalt complexes investigated by x-ray methods. It must be remembered however that factors related to the specific nature of the tripod ligand may also favor the distortion.[6] Of course, no deviation from the trigonal-bipyramidal geometry is expected for the iron complex, in which the $2a_1$ orbital is empty.

The present complexes conform to the "18-electron rule", in the sense that the number of electrons in the highest occupied molecular orbitals based largely on the metal atom does not exceed 18. This number is attained in the cobalt and nickel complexes through the formation of a lone pair on the nitrogen atom of the tripod ligand, which is removed from the coordination sphere.

As the ground state is orbitally nondegenerate in these complexes, the NO group is expected to coordinate linearly to the metal, essentially in agreement with what is found. It has been pointed out[23] that if the local symmetry of the MNO moiety belongs to point groups with no degenerate representations, as a result of distortion in the coordination, the degeneracy of the π^* acceptor orbitals of NO and similar ligands is lifted, so that the MNO group is no longer required to be linear. It is difficult to decide whether the small distortions from linearity, that are observed in the present structures, should be attributed to the above factor or to the effect of short contacts in the solid, involving the NO group.

Turning to a consideration of the electronic spectra (Table II, Figure 3), the strong band in the region 16–21 kK which is present in each case may be attributed to an essentially metal-based transition. In view of the covalent character of bonds in these complexes, such a band may be tentatively assigned, on the basis of the one-electron energy level diagram of Figure 4c, as follows: $\{MNO\}^{10}$ complexes, $^1E[2a_1 3e] \leftarrow$

${}^1A_1[2a_1{}^2]$; $\{MNO\}^9$ complex, ${}^2E[3e] \leftarrow {}^2A_1[2a_1]$; $\{MNO\}^8$ complex, ${}^1E[2e^3 2a_1] \leftarrow {}^1A_1[2e^4]$. The insensitivity of this band to substitution of the phosphorus by arsenic donor atoms in the $\{MNO\}^{10}$ complexes (Table II) may be understood in view of the nature of the "nonequatorial" orbitals essentially involved in the transition. The shift to lower frequencies of the absorption for the $\{MNO\}^9$ cobalt complex compared to that for the nickel complex (Table II, Figure 3) may be caused by the smaller amount of tetrahedral distortion in the former and by the different energies of d orbitals of the two metals (Co > Ni). The absorption at ca. 6.8 kK, which is found only in the spectrum of the $\{MNO\}^9$ cobalt complex (Figure 3), could be assigned as ${}^2E[2e^3 2a_1{}^2] \leftarrow {}^2A_1[2e^4 2a_1]$ and its low intensity might be attributed to the distance from the charge-transfer region. In accordance with the assignment made for the $\{MNO\}^8$ complexes, the band at ca. 20 kK in the spectrum of the iron compound undergoes a hypsochromic shift when the apical nitrogen of the np_3 ligand is substituted by a phosphorus atom, in the complex $[Fe(NO)(pp_3)]BPh_4$.[19]

A shoulder or splitting of the band similar to that observed in the spectra of the $\{MNO\}^{10}$ complexes (Figure 3, Table II) is also found for the related nickel complexes formed with different ligands.[21,22] On the other hand, no splitting is observed for the $\{MNO\}^9$ complex $[Co(NO)(np_3)]BPh_4$ (Figure 3). This feature of the spectra of the $\{MNO\}^{10}$ species could be attributed to an effect of configuration interaction involving the low-lying $3d^9 4s$ excited configuration of the metal[24] or to the appearance of the spin-forbidden transition to the triplet state originating from the $2a_1 3e$ excited configuration (Figure 4c) of the $\{MNO\}^{10}$ complexes. This transition may borrow intensity from the spin-allowed one, via spin-orbit mixing of the E components of the two excited states of different spin multiplicity, belonging to the $2a_1 3e$ configuration. Appreciable mixing should occur, as the different spin states are close in energy when there is extensive delocalization, as in these covalent complexes.[25] The importance of this sort of mechanism in isocyanide complexes has been supported by MCD studies.[26]

The NO stretching frequencies for the nickel complexes are higher than that for the complex $[Co(NO)(np_3)]BPh_4$ (Table I). The lower NO bond order, i.e., higher π^*(NO)-orbital occupancy in the cobalt complex, may be attributed to the higher d-orbital energy in the latter, which favors back-donation from the metal to the nitrosyl group. The very low ν(NO) value in the neutral $[Co(NO)(np_3)]$ complex is rationalized by the same argument. However, these considerations do not explain the rather high 1700-cm^{-1} frequency for the iron complex in Table I which is close to the 1690-cm^{-1} value found for the related complex[19] $[Fe(NO)(pp_3)]BPh_4$. Conceivably, the increased M–N(NO) bond distance in the five-coordinate complexes [1.67 (1) Å in the complex of ref 19, compared to 1.59 (1) Å in **3**] reduces the amount of back-donation to the NO group.[27]

Acknowledgment. Thanks are due to Mr. F. Zanobini for technical assistance and to Messrs. F. Nuzzi and G. Vignozzi for microanalyses.

Registry No. $[Ni(NO)(np_3)]I$, 58816-92-5; $[Ni(NO)(np_3)]NO_3$, 58816-94-7; $[Ni(NO)(np_3)]BF_4$, 58816-95-8; $[Ni(NO)(np_3)]BPh_4$, 58816-96-9; $[Ni(NO)(nas_3)]I$, 58816-97-0; $[Ni(NO)(nas_3)]BPh_4$, 58816-99-2; $[Co(NO)(np_3)]$, 58817-00-8; $[Co(NO)(np_3)]BPh_4$, 58817-02-0; $[Fe(NO)(np_3)]BPh_4$, 58817-04-2; $[NiI(np_3)]$, 54353-75-2; $[Ni(NO_3)(np_3)]$, 52951-35-6; $[NiI(nas_3)]$, 57287-15-7; $[CoH(np_3)]$, 53687-39-1; $[Ni(np_3)]$, 52633-73-5.

Supplementary Material Available: Listings of structure factor amplitudes (16 pages). Ordering information is given on any current masthead page.

References and Notes

(1) J. H. Enemark and R. D. Feltham, *Coord. Chem. Rev.*, **13**, 339 (1974); R. Hoffmann, M. M. L. Chen, M. Elian, A. R. Rossi, and D. M. P. Mingos, *Inorg. Chem.*, **13**, 2666 (1974), and references therein.

(2) L. Sacconi, *Coord. Chem. Rev.*, **8**, 351 (1972); R. Morassi, I. Bertini, and L. Sacconi, *ibid.*, **11**, 343 (1973).

(3) L. Sacconi, J. J. Van der Zee, K. G. Shields, and C. H. L. Kennard, *Cryst. Struct. Commun.*, **2**, 229 (1973).

(4) (a) P. Dapporto and L. Sacconi, *J. Chem. Soc. A*, 1804 (1970); (b) C. Mealli, P. L. Orioli, and L. Sacconi, *ibid.*, 2691 (1971).

(5) (a) M. Di Vaira and A. Orlandini, *J. Chem. Soc., Dalton Trans.*, 1704 (1972); (b) L. Sacconi, C. A. Ghilardi, C. Mealli, and F. Zanobini, *Inorg. Chem.*, **14**, 1380 (1975).

(6) (a) M. Di Vaira and A. Orlandini, *Inorg. Chem.*, **12**, 1292 (1973); (b) M. Di Vaira, *J. Chem. Soc., Dalton Trans.*, 1575 (1975).

(7) M. Di Vaira, C. A. Ghilardi, and L. Sacconi, Atti VIII Convegno Associazione Italiana Chimica Inorganica, 1975, No. C7.

(8) L. Sacconi and I. Bertini, *J. Am. Chem. Soc.*, **90**, 5443 (1968).

(9) L. Sacconi, I. Bertini, and F. Mani, *Inorg. Chem.*, **7**, 1417 (1968).

(10) L. Sacconi, I. Bertini, and F. Mani, *Inorg. Chem.*, **6**, 262 (1967).

(11) L. Sacconi, A. Orlandini, and S. Midollini, *Inorg. Chem.*, **13**, 2850 (1974).

(12) L. Sacconi, P. Dapporto, and P. Stoppioni, *Inorg. Chem.*, **15**, 325 (1976).

(13) C. A. Ghilardi, S. Midollini, and L. Sacconi, *Inorg. Chem.*, **14**, 1790 (1975).

(14) J. M. Stewart, F. A. Kundall, and J. C. Baldwin, Ed., "X-Ray 72", Technical Report TR 192, University of Maryland, 1972.

(15) C. K. Johnson, Report ORNL 3794, Oak Ridge National Laboratory, Oak Ridge, Tenn., 1965.

(16) D. T. Cromer and J. A. Waber, *Acta Crystallogr.*, **18**, 104 (1965).

(17) R. F. Stewart, E. R. Davidson, and W. T. Simpson, *J. Chem. Phys.*, **42**, 3175 (1965).

(18) D. T. Cromer, *Acta Crystallogr.*, **18**, 17 (1965).

(19) While this work was in progress, we have determined the structure of the $[Fe(NO)(pp_3)]BPh_4$ complex formed with the tripod ligand tris(2-diphenylphosphinoethyl)phosphine, pp_3, which differs from np_3 by substitution of nitrogen with a phosphorus atom; the coordination in $[Fe(NO)(pp_3)]BPh_4$ is closely similar to that in $[Fe(NO)(np_3)]BPh_4$ [M. Di Vaira, A. Tarli, P. Stoppioni, and L. Sacconi, *Cryst. Struct. Commun.*, **4**, 653 (1975)].

(20) D. M. P. Mingos and J. A. Ibers, *Inorg. Chem.*, **10**, 1479 (1971); C. G. Pierpont and R. Eisenberg, *ibid.*, **11**, 1094 (1972).

(21) J. H. Meiners, C. J. Rix, J. C. Clardy, and J. G. Verkade, *Inorg. Chem.*, **14**, 705 (1975).

(22) B. Berglund and D. W. Meek, *Inorg. Chem.*, **11**, 1493 (1972).

(23) S. F. A. Kettle, *Inorg. Chem.*, **4**, 1661 (1965); J. H. Enemark, *ibid.*, **10**, 1952 (1971).

(24) J. C. Slater, "Quantum Theory of Atomic Structure", Vol. I, McGraw-Hill, New York, N.Y., 1960, Chapter 16.

(25) A. B. P. Lever, "Inorganic Electronic Spectroscopy", Elsevier, Amsterdam, 1968, p 241.

(26) S. B. Piepho, P. N. Schatz, and A. J. McCaffery, *J. Am. Chem. Soc.*, **91**, 5994 (1969); H. Ishi and W. R. Mason, *Inorg. Chem.*, **14**, 913 (1975).

(27) After the manuscript for this article had been submitted, an empirical treatment of the NO stretching vibrations was published: B. L. Haymore and J. A. Ibers, *Inorg. Chem.*, **14**, 3060 (1975). According to their empirical rules, which apply to even-electron complexes, the corrected NO stretching frequency for our nickel complex falls in the range of the linear MNO group. That for the iron complex belongs to the range of the bent MNO group but it is close to the borderline between the two ranges.